Self-adaptive mesoporous CoS@alveolus-like carbon yolk-shell microsphere for alkali cations storage

Qidong Li, Li Li, Kwadwo Asare Owusu, Wen Luo, Qinyou An, Qiulong Wei, Qingjie Zhang, Liqiang Mai

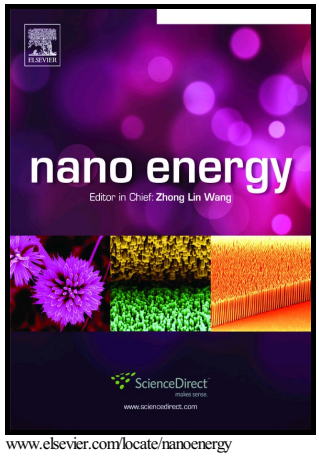

www.elsevier.com/locate/nanoenergy

PII: S2211-2855(17)30560-8
DOI: http://dx.doi.org/10.1016/j.nanoen.2017.09.022
Reference: NANOEN2198

To appear in: *Nano Energy*

Received date: 27 July 2017
Revised date: 31 August 2017
Accepted date: 10 September 2017

Cite this article as: Qidong Li, Li Li, Kwadwo Asare Owusu, Wen Luo, Qinyou An, Qiulong Wei, Qingjie Zhang and Liqiang Mai, Self-adaptive mesoporous CoS@alveolus-like carbon yolk-shell microsphere for alkali cations storage, *Nano Energy,* http://dx.doi.org/10.1016/j.nanoen.2017.09.022

Self-adaptive mesoporous CoS@alveolus-like carbon yolk-shell microsphere for alkali cations storage

Qidong Li,[a#] Li Li,[a#] Kwadwo Asare Owusu,[a] Wen Luo,[ab] Qinyou An,[a] Qiulong Wei,*[ac] Qingjie Zhang[a] and Liqiang Mai*[ad]

[a] State Key Laboratory of Advanced Technology for Materials Synthesis and Processing, International School of Materials Science and Engineering, Wuhan University of Technology, Wuhan 430070, China. E-mail: mlq518@whut.edu.cn.

[b] Laboratoire de Chimie et Physique: Approche Multi-échelles des Milieux Complexes, Institut Jean Barriol, Université de Lorraine, 57070 Metz, France.

[c] Department of Materials Science and Engineering, University of California Los Angeles, CA 90095-1595, USA. E-mail: qlwei@ucla.edu.

[d] Department of Chemistry, University of California, Berkeley, California 94720, United States.

[#] These authors contributed equally to this work.

Abstract

To address the severe volume changes of transition metal chalcogenides that results in inferior cycling performance, herein, a unique yolk-shell microsphere composed of mesoporous cobalt sulfide yolk and alveolus-like carbon shell (M-CoS@C) is constructed. The mesoporous CoS yolks possess large surface area (46.3 m^2 g^{-1}) accompanied with the interconnected mesoporous structure, which provides a large contact area to facilitate the permeation of the electrolyte and shorten the ion diffusion path. The alveolus-like carbon shells provide enough void spaces and highly self-adaptive structure to ensure the high stability of the electrode. Owing to the multifunctionality of this unique structure, the M-CoS@C electrode shows impressive cycling stability (790 mAh g^{-1} after 500 cycles at 1 A g^{-1} for Li-storage, 532 mAh g^{-1} after 100 cycles at 0.2 A g^{-1} for Na-storage) and excellent rate capability (330 mAh g^{-1} at 20 A g^{-1} for Li-storage, 190 mAh g^{-1} at 20 A g^{-1} for Na-storage). This unique mesoporous yolks@alveolus-like carbon shell structure and the self-sacrificing synthesis method present the effective strategies to promote the utilization of transition metal chalcogenides for practical applications.

Keywords: self-adaption; yolk-shell structure; cobalt sulfide; high performance; alkali cations storage

1. Introduction

In order to address the shortage of green energy and emissions of carbon oxides, many efforts have been devoted to innovating the high-efficiency and environment-friendly energy storage systems. Among the various energy storage systems, the market is hugely dominated by lithium-ion batteries (LIBs) due to their outstanding features which include high energy density, high power density, and long lifespan.[1] Recently, sodium-ion batteries (SIBs) are fast-becoming another promising storage device for large-scale energy storage systems due to the low cost and abundant resources of sodium when compared to lithium.[2-4] The both two energy storage technologies have their own application fields, however, the state-of-the-art LIBs and SIBs are still unable to satisfy the ever-increasing demand of energy consumption. What's more, many high-performance anode materials for LIBs cannot be applied in SIBs because of the larger diameter of sodium ions (Li^+: 0.76 Å; Na^+: 1.02 Å).[5] Up to now, many alternative materials, including carbon-based materials, metal oxides and alloy-based materials, have been explored as potential anodes for SIBs.[6-11] Although some encouraging progresses have been made, developing appropriate anode materials with high capacity and long cycle stability still requires further research to successfully cope with the series of challenges posed by the energy crisis.

Among anode materials, transition metal chalcogenides (TMCs) have demonstrated higher reversible capacity compared to the insertion-type anode

materials, especially for SIBs.[12-15] Recently, cobalt sulfides are considered as a host material for Li^+ and Na^+ owing to their low cost and high theoretical capacity.[16, 17] However, the detrimental effect of severe volume changes makes them deliver inferior electrochemical performances, especially unsatisfied cyclability. The nanoarchitecture construction and carbon modification, such as hollow structure CoS_x and sandwich-like cobalt sulfide-graphene composites, have been used to improve their electrochemical performances.[17-19] Nevertheless, the construction of their self-structure and the decoration with open carbon system were unable to fully overcome the essential issue of the severe volume changes. It has been demonstrated that the confined structure, such as yolk-shell carbon-coated structure, is extremely effective at improving the stability of the electrodes.[20-26] Two key points must be considered in constructing an effective yolk-shell carbon-coated structure: i) adequate void space for the expansion of the yolk during cycling process; ii) appropriate thickness of the carbon shell to ensure robust mechanical properties and fast kinetics. Therefore, predictably, a controlled yolk-shell structure will effectively improve the electrochemical performances of cobalt sulfides, which has great significance for promoting the practical applications of large-volume-change anode materials.

In this manuscript, we have successfully explored an ingenious method to synthesize a unique yolk-shell microsphere composed of mesoporous cobalt sulfide yolk and alveolus-like carbon shell (M-CoS@C) for the very first time. The mesoporous CoS (M-CoS) yolks with an average pore size of ~15 nm offer large electrode/electrolyte contact areas and short diffusion paths for electron and ions. The

alveolus-like carbon shells provide a spatially confined structure to guarantee the integrity of the yolk during cycling process. Owing to the multifunctionality of the M-CoS@C structure, the M-CoS@C electrode shows impressive cycling stability and excellent rate capability for Li^+ and Na^+ storage.

2. Experimental section

2.1 *Experimental Methods.*

Synthesis of the precursor: The precursor was synthesized through a room-temperature solvent method. Specifically, $Co(NO_3)_2 \cdot 6H_2O$ (3 mmol) and thioacetamide (TAA, 15 mmol) were dissolved in ethyl alcohol (40 mL) under stirring for 0.5 h. The obtained wine-red solution was allowed to stand at room-temperature for 5days. The precursor was collected after washing with three times of ethyl alcohol and then dried under vacuum at 80 °C overnight for further use.

Synthesis of the precursor@SiO_2 microspheres: The as-synthesized precursor (300 mg) obtained above was well dispersed in a mixed solvent that is composed of ethyl alcohol (35mL) and deionized water (5 mL) with the assistance of ultrasonication (0.5 h) and stirring (0.5 h). Then, NH_4OH solution (0.7 mL) and tetraethyl orthosilicate (0.2 mL) were added to the above suspension and stirring for another 4 h at room-temperature. The core-shell precursor@SiO_2 microspheres were collected and washed three times with ethyl alcohol.

Synthesis of the yolk-shell M-CoS@C: The obtained precursor@SiO_2 microspheres were dispersed in mixed solvent that composed of ethyl alcohol (35 mL) and deionized water (5 mL) without drying. After 0.5 h stirring, resorcinol (150 mg) and NH_4OH solution (1.5 mL) were added sequentially and stirred for another 10 min. Then, formalin (F, 0.21 mL) was finally added. After continually stirring for 24 h, the obtained precursor@SiO_2@RF microspheres were collected and washed three times with ethyl alcohol. The yolk-shell M-CoS@SiO_2@C was prepared by annealing of the precursor@SiO_2@RF powder at 600 °C for 4 h in vacuum. Finally, the silica layer

was etched away by the HF solution (5 wt.%), and the yolk-shell M-CoS@C microspheres were obtained. A control sample was synthesized by following the same procedures, whiles adjusting the resorcinol and formalin to 200 mg and 0.28 mL, respectively (denoted as M-CoS@C-200).

2.2 Materials Characterization.

Scanning electron microscopy (SEM) images were collected with a JEOL-7100F microscope (accelerating voltage 20 kV). Transmission electron microscopy (TEM) and high-resolution TEM (HRTEM) images, and corresponding element mapping analyses were recorded by using a JSM-2010 microscope. X-ray diffraction (XRD) patterns were obtained on a D8 Advance X-ray diffractometer, using Cu-Kα radiation (λ = 1.5418 Å). Fourier transform infrared spectroscopy (FTIR) spectra were obtained using a Nexus system. Raman spectra were collected by a Renishaw INVIA micro-Raman spectroscopy system. BET surface areas were measured using Tristar II 3020 instrument by nitrogen adsorption of at 77 K. Thermogravimetric analysis (TGA) was performed using a Netzsch STA 449 F5 simultaneous analyzer and the sample was heated from room temperature to 800 °C in Ar and air with a heating rate of 10 °C min^{-1}.

2.3 Electrochemical measurements.

The working electrodes were prepared by mixing 80 wt.% active material, 15 wt.% acetylene black and 5 wt.% carboxyl methyl cellulose (CMC) binder. The slurry was cast onto Ti foil by using a doctor blade and dried in a vacuum oven at 70 °C for 8 h. The mass loading of active materials was 1.0 mg cm^{-2}. Then, the electrochemical properties were characterized by assembling 2016 coin cells with Li/Na foils as the

anode. During the assembly process, a 1 M of $LiPF_6$ in ethylene carbonate (EC) and dimethyl carbonate (DMC) (1:1, vol.%) was used as an electrolyte for LIBs testing. Alternatively, a 1 M of $NaClO_4$ in propylene carbonate (PC) with 5 wt.% of FEC served as the electrolyte for SIBs testing. A volume of 100 μL electrolyte was added for each coin cell. Galvanostatic charge/discharge measurements were performed using a multichannel battery testing system (LAND CT2001A). Cycling voltammetry (CV) and electrochemical impedance spectroscopy (EIS) were collected with an Autolab potentiostat/galvanostat at original open circuit potential at room temperature. The EIS measured from 0.01 Hz–100 kHz.

3. Results and Discussion

The M-CoS@C yolk–shell structures were synthesized as shown schematically in **Figure 1a** (see Methods section for details). First, the precursor with microsphere morphology (diameter range between 1~5 μm) was prepared at room temperature (**Figure 1b, f, and Figure S1**). Second, a layer of condensed silica was coated on the precursor microsphere *via* the conventional Stöber method, followed by coating with a polymeric layer of resorcinol-formaldehyde (RF). Then the intermediate product was annealed at 600 °C under vacuum to obtain the M-CoS@SiO_2@C. Finally, the silica layer was etched by dilute HF to form the M-CoS@C. The precursor plays a vital role in the construction of M-CoS@C. Owing to the large size of the precursor, the SiO_2 layer forms protuberances on the surface of the precursor microsphere (**Figure 1a,c, and g**).[27] Moreover, the energy dispersive X-ray (EDX) analysis and elements mapping show the uniform distribution of S and Co in the precursor with a

high atomic ratio of S:Co (about 4.6:1 as shown in **Figure S1a-e**). FTIR spectra of thioacetamide, the precursor and CoS are compared in **Figure S1f**. The results demonstrate that the precursor is a Co-thioacetamide complexes. The excess S in the precursor evaporated during the carbonization process, which resulted in a remarkable weight loss (**Figure S1g**) and led to drastic volume contraction and the formation of a mesoporous yolk (**Figure 1a**). **Figure S2** displays the morphology of the M-CoS. After calcination, the sphere structure was maintained with a rough surface (**Figure S2a,b**). The TEM and high-angle annular dark field (HAADF) images clearly show the mesoporous feature of the M-CoS (**Figure S2c,d**). The diameter of the core reduced from 2.2 to 1.5 μm during the calcination process (**Figure 1h**), indicating that the self-sacrificing generated void space can withstand at least 215% of the volume expansion of the CoS yolk, excluding the space of SiO_2 and mesopores. The theoretical volume changes of CoS during cycling process when used for Li/Na storage can be estimated according to the conversion reaction[28]:

$$CoS + 2Li/Na \rightarrow Co + Li_2S/Na_2S$$

The volume variation is calculated to be ~105% for Li-storage ($V_{CoS} = M_{CoS}/\rho_{CoS}$ = 16.7 cm^3, V_{Co} = 6.62 cm^3, V_{Li2S} = 27.68 cm^3) and ~191% (V_{Na2S} = 41.96 cm^3) for Na-storage,[20] which can be easily accommodated by the void space. The SEM and TEM images exhibit that the M-CoS yolk is well confined by an alveolus-like carbon shell (**Figure 1e,i**). The thickness of the carbon shell is about 23 nm, as shown in the inset of **Figure 1i**. However, without the pre-coated SiO_2, the RF layer were unable to uniformly coat on the precursor spheres (**Figure S3**), demonstrating the indispensable

role of SiO_2 layer for the construction of M-CoS@C.

As depicted in the XRD patterns of the three samples, the precursor exhibits an amorphous feature (**Figure 2a**). All diffraction peaks of the M-CoS and M-CoS@C can be indexed to hexagonal CoS with lattice constants a = 3.368 Å, c = 5.170 Å (JCPDF 03-065-3418) without impurity, indicating the precursor has been totally transformed into CoS after calcination. No diffraction peak of the carbon shell can be detected because of its amorphous feature. Raman spectra were used to analyze the property of the carbon shell, as shown in **Figure 2b**. Two peaks centred at 1348 and 1587 cm^{-1} can be observed for the yolk-shell M-CoS@C, corresponding to the D-band (disorder-induced) and G-band (graphitic) of carbon.[29] The carbon content of the M-CoS@C is estimated to be 29.5%, according to the thermogravimetric analysis results (**Figure S4**). The pore structure of the three samples was examined by N_2 adsorption/desorption technique (**Figure 2c,d**). The N_2 adsorption/desorption isotherm of the precursor shows no pores in the precursor and its BET specific surface area is 0.8 $m^2 g^{-1}$. The isotherm of M-CoS can be indexed to type IV isotherm with H1 type hysteresis loops, which demonstrates that the M-CoS possesses interconnected pores with narrow size distributions.[30] The BJH adsorption pore distribution plot of M-CoS depicts that its pore sizes mainly concentrate on ~15 nm, which well coincide with the isotherm and TEM image (**Figure 2d**). The BET specific surface area of M-CoS is estimated to be 46.3 $m^2 g^{-1}$, which is much higher than that of the precursor. Such large surface area accompanied with the interconnected mesoporous structure effectively provide a large contact area to facilitate the permeation of the electrolyte

and shorten the ion diffusion path. After constructing the yolk-shell structure, the M-CoS@C shows an IV isotherm with H2 type hysteresis loops, resulting from the large void space confined by the carbon shell which is similar to the 'ink bottle' pores.[30] The BET specific surface area is increased to 166.2 m^2 g^{-1} because of the carbon shell. The pore sizes of M-CoS@C concentrate on ~3.5 and ~15 nm, corresponding to the pores of carbon shell and CoS yolk, respectively. The HAADF image of the M-CoS@C shows that the CoS yolk possesses a rough surface similar to M-CoS, indicating the mesoporous structure was well maintained after carbon coating. The HRTEM image in the inset of **Figure 2e** clearly displays a set of parallel fringes with *d*-spacing of 0.17 nm, corresponding to the (110) plane of CoS. Moreover, the elements mapping of the yolk-shell M-CoS@C demonstrate that the CoS yolk is totally confined by the alveolus-like carbon shell with a large void space (**Figure 2f-g**). All these results verify that mesoporous CoS encapsulated by alveolus-like carbon in a yolk-shell structure has been successfully fabricated.

The electrochemical lithium storage properties of both the yolk-shell M-CoS@C and M-CoS microspheres are compared in **Figure 3**. Cyclic voltammogram (CV) was first used to analyse the redox process of the samples during cycling. It is clearly shown that the reduction peak of M-CoS@C at 0.35 V is much higher than that of the M-CoS at the first discharge process (**Figure 3a,b**). This can be explained by the formation of more SEI due to the carbon shell. The following cycles exhibit two oxidation peaks (2.09 and 2.38 V) and two reduction peaks (1.30 and 1.73 V), which is similar to previously reported hierarchical CoS_x (Co:S ≈ 1:0.9).[18] This result

demonstrates that the redox processes after the first cycle are related to the ratio of cations and anions in the materials instead of the components for conversion type materials. Interestingly, M-CoS@C shows an activation process accompanied with the increase of capacity and decrease of polarization (**the blue arrow in Figure 3a**). On the contrary M-CoS shows an obviously increased polarization and decreased capacity based on the CV curves (**the red arrow in Figure 3b**), which is attributed to its sluggish kinetics resulting from the pulverization of the electrode. **Figure 3c** displays the comparison of the cycling performances of M-CoS@C (the capacities are calculated based on the mass of the composite) and M-CoS. It is manifested that the yolk-shell M-CoS@C electrode delivers much better stability than that of M-CoS. Even after 500 cycles at 1 A g^{-1}, the M-CoS@C still displays a high reversible capacity of 790 mAh g^{-1}, much higher than that of M-CoS (322 mAh g^{-1}). Particularly, the capacity of M-CoS decreases from 736 to 195 mAh g^{-1} within 50 cycles because of structure deterioration, which is in well agreement with the CV results. The corresponding discharge/charge curves of the two samples are depicted in **Figure S5**. The M-CoS@C electrode exhibits stable discharge/charge curves with obvious charge-discharge platforms after 500 cycles, indicating a highly stable structure (**Figure S5a**). On the contrary, the platforms of M-CoS electrode totally disappear after 50 cycles, indicating the deactivation of CoS owing to the sluggish kinetics (**Figure S5b**). Furthermore, the rate performances of each sample were further investigated at various current densities ranging from 0.1 to 20 A g^{-1} (**Figure 3d,e**). The M-CoS exhibits higher capacity than the M-CoS@C during the first few cycles at

0.1 A g^{-1} due to the carbon component in the M-CoS@C. Beyond that, the M-CoS@C electrode delivers capacities of 880, 835, 795, 715, 600, 485, and 330 mAh g^{-1} at 0.2, 0.5, 1, 2, 5, 10, and 20 A g^{-1} respectively, which is much higher than that of the M-CoS electrode (**Figure 3d**). Furthermore, when the rate is directly reduced again to 0.2 A g^{-1}, the M-CoS@C electrode recovers a capacity of 920 mAh g^{-1}, which is higher than that of the first few cycles. This is due to the activation process similar to its cycling performance. Except for its stable structure, the high performances of the M-CoS@C electrode also benefit from the improved electronic conductivity which was confirmed by the EIS spectra (**Figure S6**). The charge transfer resistance (R_{ct}) reduced from 111 to 69 Ω after constructing the yolk-shell M- CoS@C structure. It is noteworthy that the thickness of the carbon shell, which is the crucial factor influencing its robust mechanical properties, does not translate into better performance with increasing thickness. A yolk-shell M-CoS@C electrode with a thicker carbon shell (denoted as M-CoS@C-200) was synthesized and as shown in the inset of **Figure S6b**, it shows an increased R_{ct} (149 Ω as shown in **Figure S6a**). It delivers an inferior rate performance due to increased carbon content and R_{ct}, although it shows an improved cycling stability (**Figure S6b**). All these results demonstrate that the yolk-shell M-CoS@C constructed with an appropriate carbon shell offers an extremely stable structure and increased electronic conductivity which improves the electrochemical performances of the electrode significantly.

The electrochemical sodium-storage properties of each sample are further evaluated (**Figure 4)**. The CV curve (**Figure 4a**) shows three reduction peaks (0.45,

0.85 and 1.12 V) and an oxidation peak (1.83 V) after the first cycles, indicating a conversion process similar to previous report.[18] From the CV curves, it is clearly shown that the M-CoS@C electrode possesses much better reversibility than the M-CoS (**Figure 4a and Figure S7a**). The cycling performances of the two samples at 0.2 A g^{-1} are shown in **Figure 4b**. After 100 cycles at 0.2 A g^{-1}, a high reversible capacity of 532 mAh g^{-1} still can be obtained for the M-CoS@C electrode, corresponding to a capacity retention of 87.2% (relative to that of the second cycle). Even at a high rate of 1 A g^{-1}, the M-CoS@C electrode also shows an impressive cyclability (**Figure S7b**). On the contrary, the capacity of M-CoS decreases rapidly to 55 mAh g^{-1} within 5 cycles. Its corresponding discharge/charge curves show that the platform of M-CoS is almost non-existents at the 3rd cycle, which indicates that the structure deterioration has a larger impact on the SIBs due to the larger diameter of Na^+ (**Figure S7d**). Furthermore, the yolk-shell structure also endows the M-CoS@C electrode with impressive rate capability with capacities of 635, 570, 530, 490, 440, 360, 295, and 190 mAh g^{-1} at 0.1, 0.2, 0.5, 1, 2, 5, 10, and 20 A g^{-1} respectively (**Figure 4c,d**). When the current density return back to 0.2 A g^{-1}, the capacity recovers to 570 mAh g^{-1} with an overlapped discharge/charge curves, indicating a superior stability of the yolk-shell structure (**Figure 4d**).

Figure S8 shows the XRD pattern and TEM image of the CoS electrode after discharging to 0.01 V (vs. Li^+/Li). The XRD pattern confirms the existence of Co (JCPDF 00-015-0806) and Li_2S (JCPDF 01-077-2145) at the fully discharged state of CoS electrode (**Figure S8a**). The HRTEM image in the inset of **Figure S8b** clearly

displays a set of parallel fringes with *d*-spacing of 0.2 nm, corresponding to the (111) plane of Co. These results confirm the conversion reaction between CoS and Li. To verify the influence of the structure on the electrochemical performances, ex-situ SEM images of the electrodes applied in LIBs at different cycles at full-charge state were acquired (**Figure 5**). It is clearly shown that, after 10 cycles, the particles of M-CoS break into two pieces because of the large volume change during cycling processes. After 50 cycles, the particles are totally pulverized along with the rapid capacity fading. On the contrary, the yolk-shell M-CoS@C exhibits very good integrity even after 50 cycles, demonstrating an excellent stability of the M-CoS@C electrode. The schematics of the morphological changes of these two samples are illustrated in **Figure 5b**. The M-CoS particle undergoes an uncontrolled volume expansion during the discharge process, resulting in the fracture of the particle. During charge process, the fragments of the particle shrink and separate from each other, leading to the pulverization and deactivation of the electrode.[31] After constructing the unique yolk-shell structure, the alveolus-like carbon shell confines the volume expansion of the M-CoS particle during the discharge process, which is similar to the expansion of alveolus during respiration process. This phenomena demonstrate the unique alveolus-like shell is able to effectively trap the huge volume changes of active materials, which improves the cycling stability greatly.

The ex-situ TEM image depicts that, after 50 cycles, the alveolus-like carbon shell still maintains a good integrity with an increased thickness of 43 nm due to the formation of SEI layer (**Figure 6a and the inset figure**). Furthermore, the CoS yolk

is still well confined in the alveolus-like carbon shell after 50 cycles according to the elements mappings (**Figure 6b-e**). These results clearly indicate that the void spaces are large enough to accommodate the volume expansion of CoS particles during the discharge/charge process as expected. Finally, the carbon shells can improve the conductivity and help to form a stable SEI layer. Therefore, the unique yolk-shell M-CoS@C composite is capable of achieving excellent cycling stability and rate capability, both for Li-storage and Na-storage.

4. Conclusion

In summary, a unique yolk-shell M-CoS@C composite has been successfully fabricated for the first time, in which the mesoporous CoS yolks are well confined in the carbon shells. The alveolus-like carbon shells offer a highly self-adaptive structure which can trap the active materials effectively. Benefiting from this unique yolk-shell structure, the M-CoS@C electrode is able to achieve superior electrochemical performances when applied in energy storage systems. Furthermore, this self-sacrificing generated void space method can be easily extended to the low sulfur content metal chalcogenides to improve their electrochemical performances.

Acknowledgements

This work was supported by the National Key Research and Development Program of China (2016YFA0202603), the National Basic Research Program of China (2013CB934103), the Programme of Introducing Talents of Discipline to Universities (B17034), the National Natural Science Foundation of China (51521001), the

National Natural Science Fund for Distinguished Young Scholars (51425204), and the Fundamental Research Funds for the Central Universities (WUT: 2016III001, 2017III009), Prof. Liqiang Mai gratefully acknowledged financial support from China Scholarship Council (No. 201606955096).

Appendix A. Supplementary material

Supplementary data associated with this article can be found in the online version.

References

[1] B. Kang and G. Ceder, Nature, 458 (2009) 190-193.

[2] L. O. Vogt, M. E. Kazzi, E. J. Berg, S. P. Villar, P. Novák and C. Villevieille, Chem. Mater., 27 (2015) 1210–1216.

[3] S. W. Kim, D. H. Seo, X. Ma, G. Ceder and K. Kang, Adv. Energy Mater., 2 (2012) 710–721.

[4] V. Palomares, M. Casascabanas, E. Castillomartínez, M. H. Han and T. Rojo, Energy Environ. Sci., 6 (2013) 2312-2337.

[5] H. Zhu, Z. Jia, Y. Chen, N. Weadock, J. Wan, O. Vaaland, X. Han, T. Li and L. Hu, Nano Lett., 13 (2013) 3093-3100.

[6] Y. Cao, L. Xiao, M. L. Sushko, W. Wang, B. Schwenzer, J. Xiao, Z. Nie, L. V. Saraf, Z. Yang and J. Liu, Nano Lett., 12 (2012) 3783-3787.

[7] I. Hasa, R. Verrelli and J. Hassoun, Electrochim. Acta, 173 (2015) 613-618.

[8] X. Fan, J. Mao, Y. Zhu, C. Luo, L. Suo, T. Gao, F. Han, S. C. Liou and C. Wang, Adv. Energy Mater., 5 (2015) 2314-2316.

[9] L. Wei, S. Fei, C. Bommier, H. Zhu, X. Ji and L. Hu, Accounts Chem. Res., 49 (2016) 231-240.

[10] Z. Le, F. Liu, P. Nie, X. Li, X. Liu, Z. Bian, G. Chen, H. B. Wu and Y. Lu, Acs Nano, 11 (2017) 2952-2960.

[11] W. Luo, A. Calas, C. Tang, F. Li, L. Zhou and L. Mai, ACS Appl. Mater. Inter., 8 (2016) 35219-35226.

[12] K. Zhang, Z. Hu, X. Liu, Z. Tao and J. Chen, Adv. Mater., 27 (2015) 3305-3309.

[13] Q. Li, Q. Wei, W. Zuo, L. Huang, W. Luo, Q. An, V. O. Pelenovich, L. Mai and Q. Zhang, Chem. Sci., 8 (2017) 160-164.

[14] K. Zhang, M. Park, L. Zhou, G. H. Lee, J. Shin, Z. Hu, S. L. Chou, J. Chen and Y. M. Kang, Angew. Chem. Inter. Edit., 55 (2016) 12822-12826.

[15] X. Zhao, H. Wang, R. C. Massé, J. Cao, J. Sui, J. Li, W. Cai and G. Cao, J. Mater. Chem. A, 5 (2017) 7394-7402.

[16] S. Z, C. MH, D. F, S. L and F. ZW, Chem. Commun., 51 (2015) 10486-10489.

[17] Q. Zhou, L. Liu, G. Guo, Z. Yan, J. Tan, Z. Huang, X. Chen and X. Wang, Rsc Adv., 5 (2015) 71644-71651.

[18] Y. Xiao, J. Y. Hwang, I. Belharouak and Y. K. Sun, Nano Energy, 32 (2017) 320-328.

[19] Z. Lei, B. W. Hao and W. L. Xiong, Chem. Commun., 48 (2012) 6912-6914.

[20] Y. X. Wang, J. Yang, S. L. Chou, H. K. Liu, W. X. Zhang, D. Zhao and S. X. Dou, Nature Commun., 6 (2015) 8689.

[21] H. Zhang, L. Zhou, O. Noonan, D. J. Martin, A. K. Whittaker and C. Yu, Adv. Funct. Mater., 24 (2014) 4337-4342.

[22] S. Z. Wei, W. Li, J. J. Cha, G. Zheng, Y. Yang, M. T. Mcdowell, P. C. Hsu and Y. Cui, Nature Commun., 4 (2013) 1331.

[23] N. Liu, H. Wu, M. T. Mcdowell, Y. Yao, C. Wang and Y. Cui, Nano Lett., 12 (2012) 3315-3321.

[24] C. Wu, P. Kopold, P. A. Van Aken, J. Maier and Y. Yu, Adv. Mater., 29 (2017) 1604015.

[25] Z. Liu, X. Y. Yu and U. Paik, Adv. Energy Mater., 6 (2016) 1502318.

[26] X. Xia, D. Chao, Y. Zhang, J. Zhan, Y. Zhong, X. Wang, Y. Wang, Z. X. Shen, J. Tu and H. J. Fan, Small, 12 (2016) 3048-3058.

[27] Yugang, Natl. Sci. Rev., 2 (2015) 329-348.

[28] M. T. Mcdowell, Z. Lu, K. J. Koski, J. H. Yu, G. Zheng and Y. Cui, Nano Lett., 15 (2015) 1264-1271.

[29] Q. Li, Q. Wei, J. Sheng, M. Yan, L. Zhou, W. Luo, R. Sun and L. Mai, Adv. Sci., 2 (2015) 1500284.

[30] K. S. W. Sing, Pure Appl. Chem., 57 (2009) 603-619.

[31] I. Choi, J. L. Min, S. M. Oh and J. J. Kim, Electrochim. Acta, 85 (2012) 369-376.

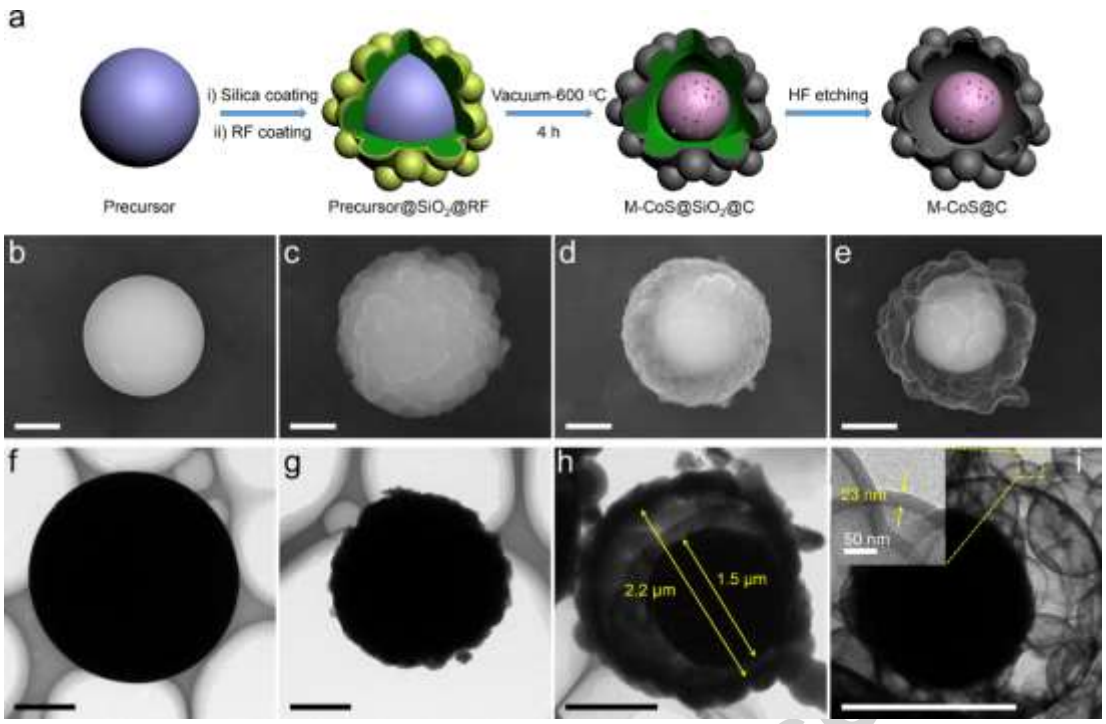

Figure 1. (a) Schematic illustration of the synthesis of yolk-shell M-CoS@C. SEM (b) and TEM (f) images of the precursor. SEM (c) and TEM (g) images of the precursor@SiO_2@RF. SEM (d) and TEM (h) images of the M-CoS@SiO_2@C. SEM (d) and TEM (h) images of the yolk-shell M-CoS@C. Scale bar, 1 μm.

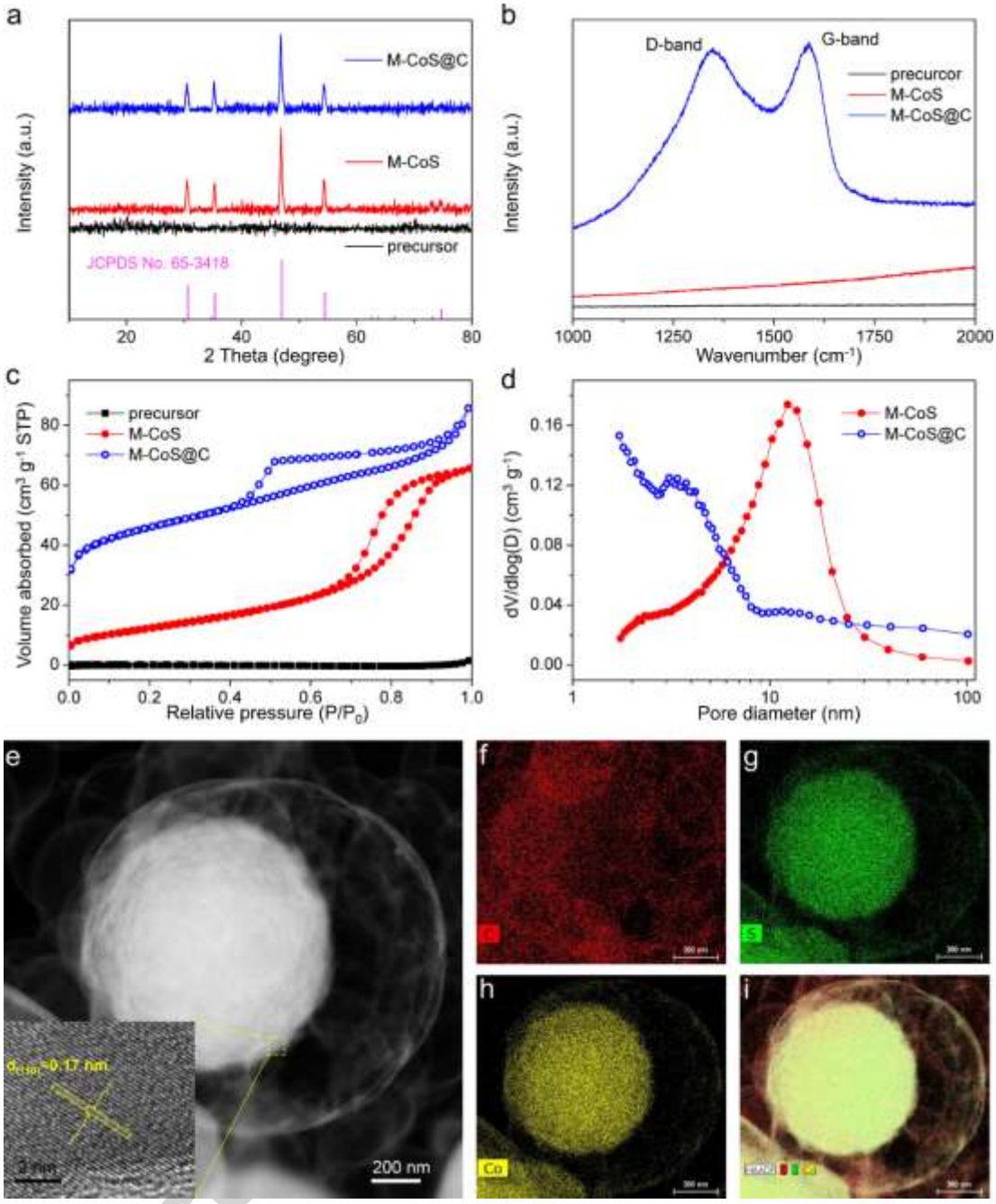

Figure 2. Physical characterization of the samples. XRD patterns (a), Raman spectra (b) and N_2 sorption isotherms (c) of the precursor, M-CoS, and yolk-shell M-CoS@C. Pore size distribution curve (d) of M-CoS and yolk-shell M-CoS@C. (e) Scanning TEM (STEM) and high-resolution TEM (inset) images of the yolk-shell M-CoS@C. (f-h) Element mapping for the yolk-shell M-CoS@C.

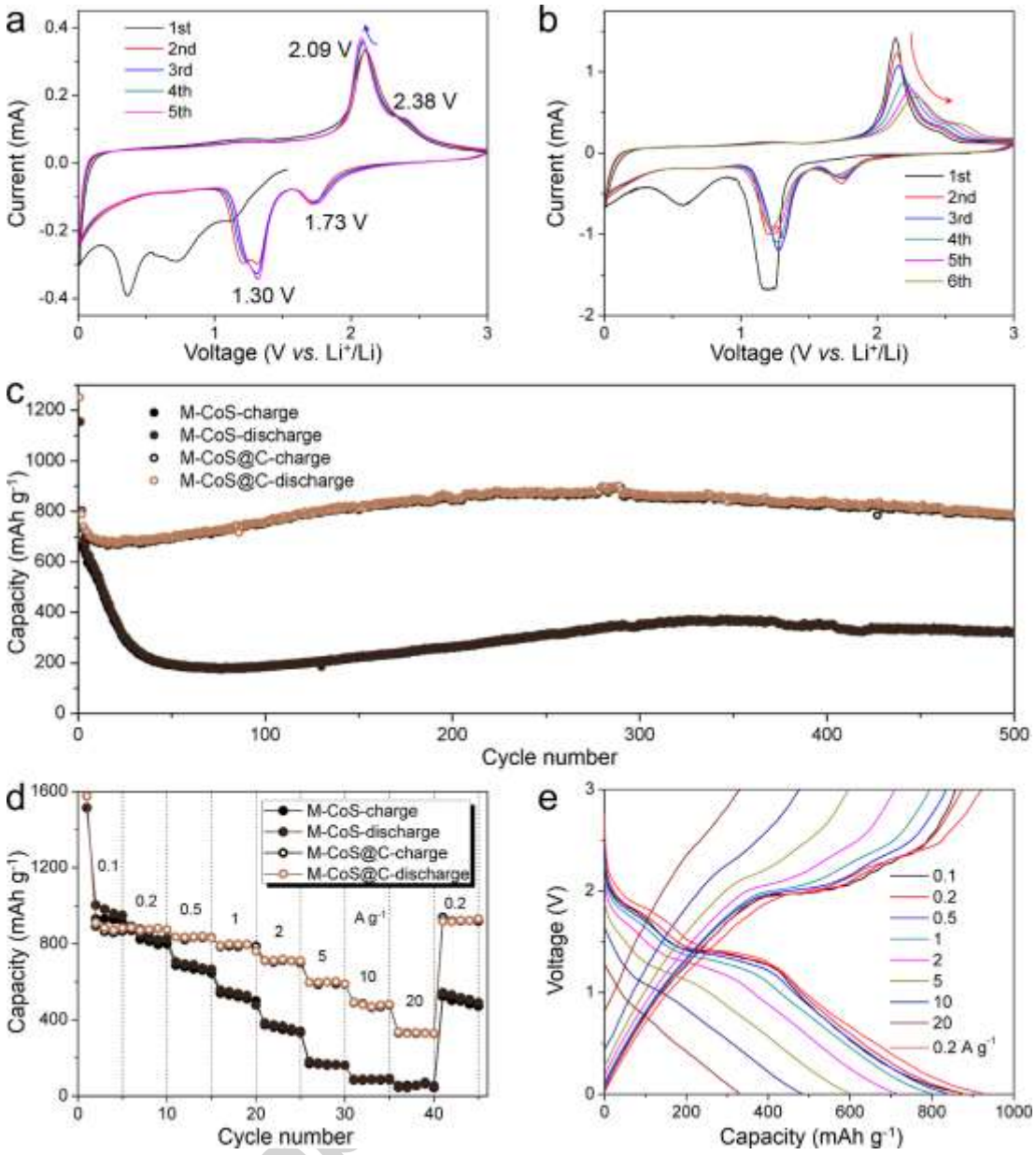

Figure 3. Electrochemical performance of the yolk-shell M-CoS@C as an anode in LIBs. Cyclic voltammograms of (a) the yolk-shell M-CoS@C and (b) M-CoS at the scan rate of 0.2 mV s^{-1} between 0.01–3 V. Cycling performances at 1 A g^{-1} (c) and rate capability (d) at various current rates of the M-CoS and the yolk-shell M-CoS@C. (e) The corresponding discharge/charge curves of the yolk-shell M-CoS@C at various current rates.

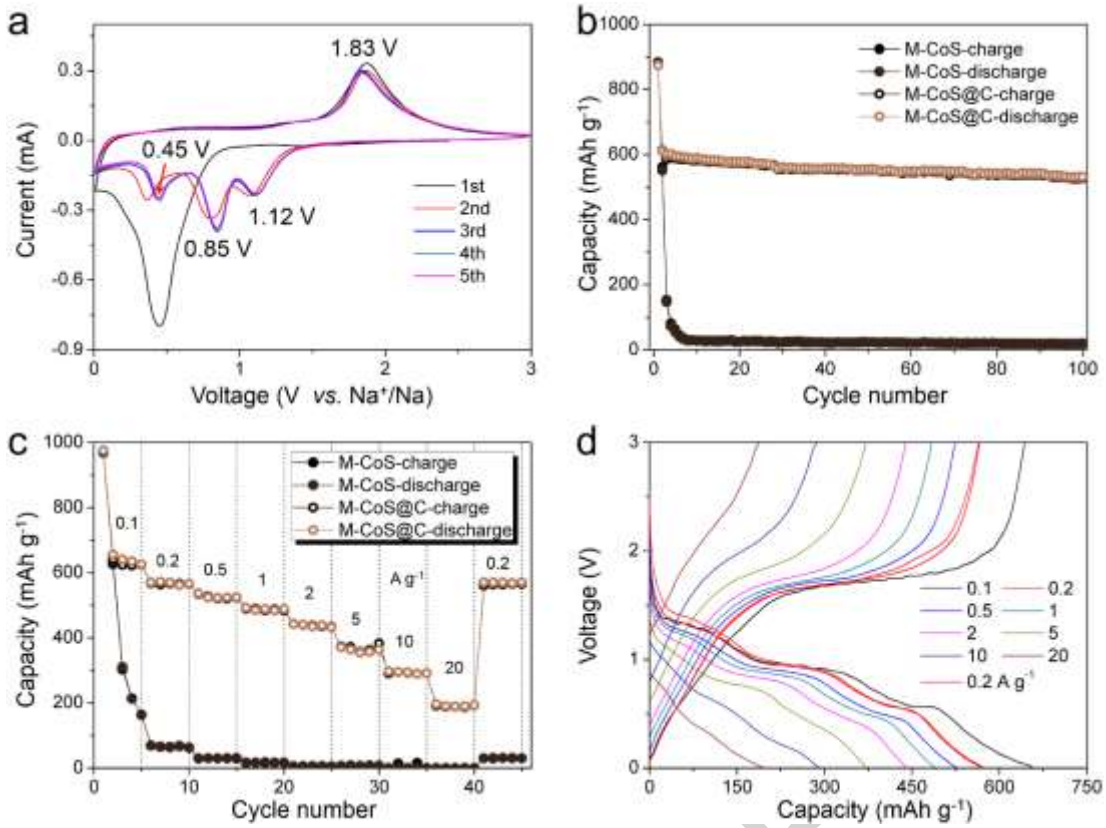

Figure 4. Electrochemical performance of the yolk-shell M-CoS@C as an anode in SIBs. (a) Cyclic voltammograms of the yolk-shell M-CoS@C at the scan rate of 0.2 mV s^{-1} between 0.01–3 V. Cycling performances at 0.2 A g^{-1} (b) and rate capability (c) at various current rates of the M-CoS and the yolk-shell M-CoS@C. (d) The corresponding discharge/charge curves of the yolk-shell M-CoS@C at various current rates.

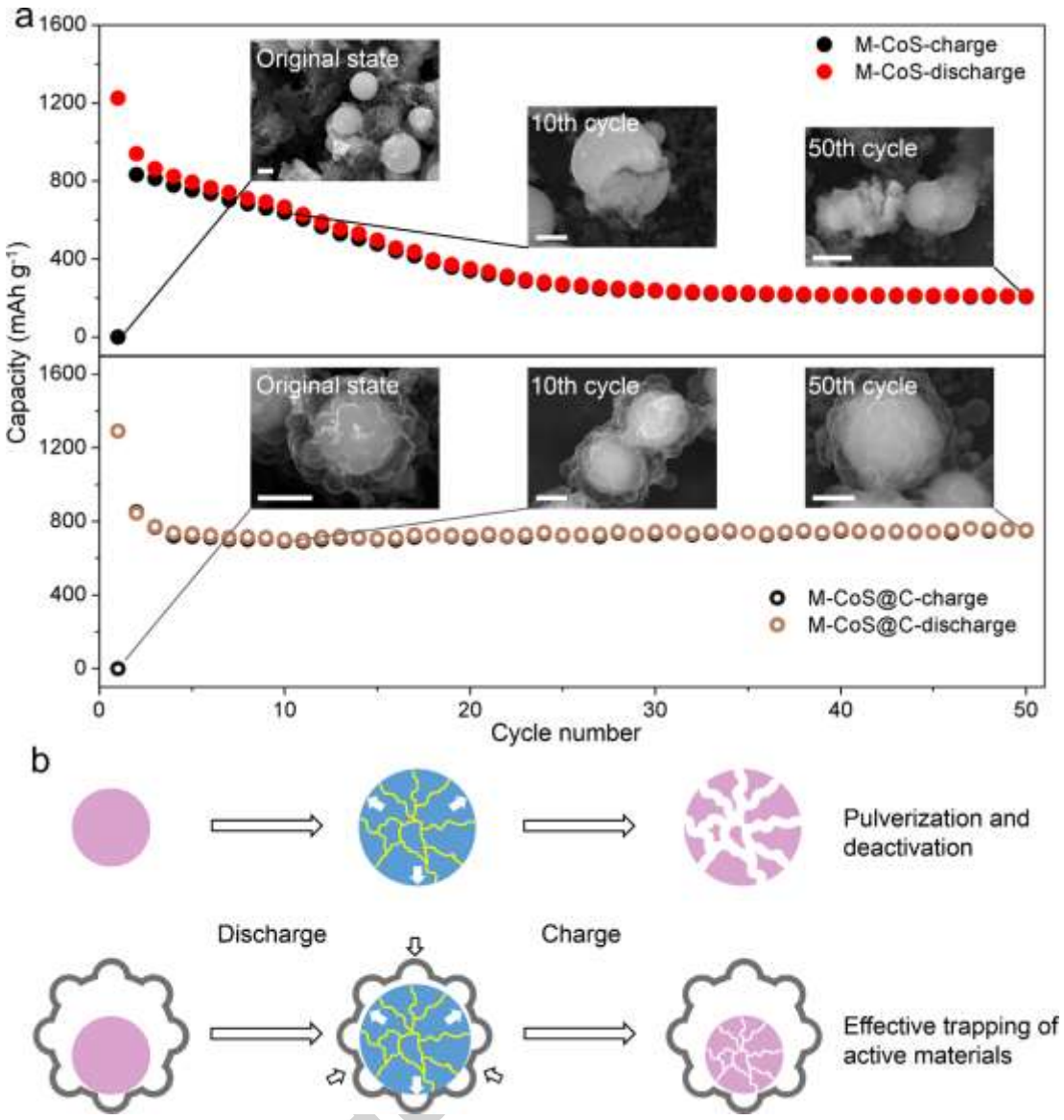

Figure 5. Morphological changes of the M-CoS and yolk-shell M-CoS@C during the cycling process. (a) The SEM images of the M-CoS and yolk-shell M-CoS@C at 0, 10th and 50th cycle (full charge state) respectively, and their corresponding cycling performances at 1 A g^{-1}. Scale bar, 1 μm. (b) Schematic of the morphological changes during the discharge/charge process.

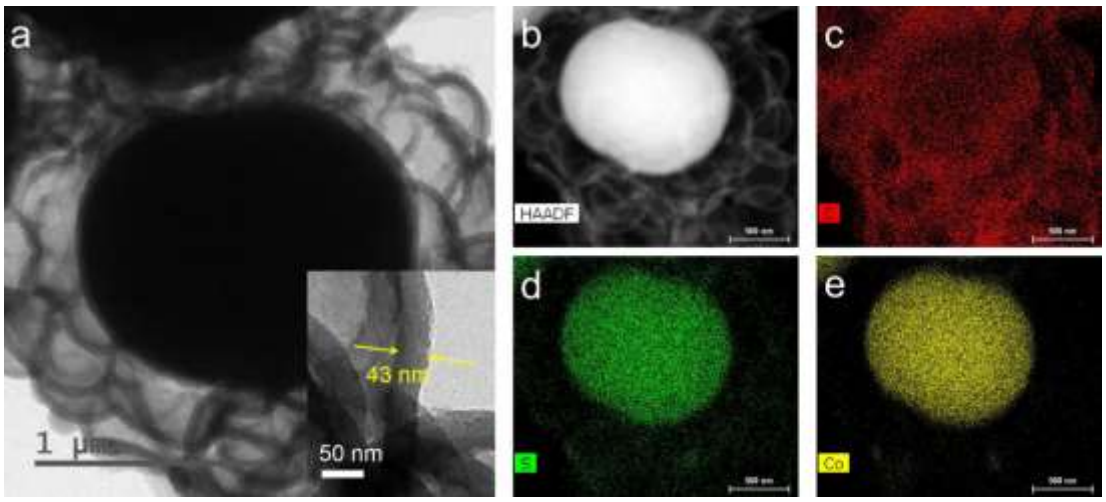

Figure 6. TEM image (a), STEM image (b) and element mapping (c-e) of the yolk-shell M-CoS@C after 50 cycles at 1 A g^{-1}.

Qidong Li received his M.S. degree in Materials Engineering from Wuhan University of Technology in 2015. He is currently working toward the Ph.D. degree and his current research focuses on the energy storage materials and devices.

Li Li is an undergraduate student and in Department of Materials Science and Engineering from Wuhan University of Technology since 2015. He has joined WUT-Harvard Joint Nano Key Laboratory for two years. His current research focuses on the electrochemical energy storage materials and devices.

Kwadwo Asare Owusu received his Master degree from Wuhan University of Technology in 2016 and is currently a Ph.D candidate in the same university under Prof. Mai Liqiang's supervision. His research interests mainly focus on the design and synthesis of nanostructed metal oxide materials for energy storage applications.

Wen Luo received her B.S. degree from Wuhan University of Technology in 2013 and she is now

a Ph.D. candidate at Wuhan University of Technology. In 2016−2017, she studies as joint training Ph.D. student at Université de Lorraine, France. Her current research focuses on advanced electrode materials for electrochemical energy storage devices.

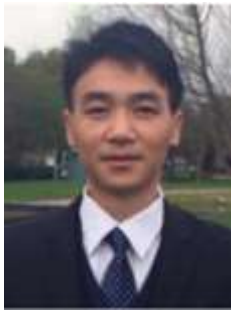

Qinyou An is Associate Professor of Materials Science and Engineering at Wuhan University of Technology (WUT). He received his Ph.D. degree from WUT in 2014. He carried out his postdoctoral research in the laboratory of Prof. Yan Yao at the University of Houston in 2014–2015. Currently, his research interest includes energy storage materials and devices.

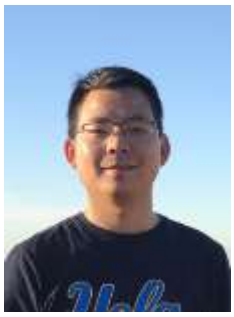

Qiulong Wei received his Ph.D. from the State Key Laboratory of Advanced Technology for Materials Synthesis and Processing, Wuhan University of Technology in 2016, under the supervision of Prof. Qingjie Zhang and Prof. Liqiang Mai. Currently, he is a postdoctoral fellow in Dunn Group at the Materials Science and Engineering department, UCLA. His current research involves the design and synthesis of nanomaterials for achieving both high energy density and power density, electrochemical energy storage devices.

Qingjie Zhang recieved his Ph.D. from Huazhong University of Science and Technology in 1990. His research focues on thermoelectric materials and related applications. At present, he is the Director of State Key Laboratory of Advanced Technology for Materials Synthesis and Processing at the Wuhan University of Technology (2005 – present) as well as the Chief Scientist of National 973 Program (2007 – 2017) in the field of thermoelectric materials.

Liqiang Mai is Chair Professor of Materials Science and Engineering at Wuhan University of Technology (WUT). He is Cheung Kong Scholar Chair Professor and the winner of the National Natural Science Fund for Distinguished Young Scholars. His current research interests focus on new nanomaterials for electrochemical energy storage and micro/nano energy devices. He received his Ph.D. degree from WUT in 2004. He carried out his postdoctoral research in the laboratory of Prof. Zhonglin Wang at Georgia Institute of Technology in 2006–2007 and worked as advanced research scholar in the laboratory of Prof. Charles M. Lieber at Harvard University in 2008–2011. He worked as advanced research scholar in the laboratory of Prof. Peidong Yang at University of California, Berkeley in 2017.

Highlights

1. Developing a self-sacrificing generated void space method to synthesize a unique yolk-shell mesoporous-CoS@C microsphere.
2. Mesoporous-CoS@C contains mesoporous CoS yolk and alveolus-like carbon shell.
3. Mesoporous-CoS@C electrode shows impressive cycling stability and excellent rate capability for both Li^+ and Na^+ storage.

Graphical abstract